Nanocomposite Hydrogels

DOI: 10.1002/anie.201206951

Periodic Mesoporous Organosilica-Based Nanocomposite Hydrogels as Three-Dimensional Scaffolds**

Nermin Seda Kehr, Eko Adi Prasetyanto, Kathrin Benson, Bahar Ergün, Anzhela Galstyan, and Hans-Joachim Galla*

Hydrogels, which are three-dimensional (3D) polymeric networks, are widely used not only as separation membranes, but also as biosensors, tissue engineering scaffolds, and drug delivery vehicles, or for stem cell cultures, owing to their stimuli responsive, hydrophilic, and biocompatible properties.[1] However, their mechanically fragile nature limits their specific uses, especially in hard-tissue-engineering applications.[2] The generation of nanocomposite (NC) hydrogels[3,4] alters this situation. NC hydrogels are organic–inorganic nanocomposites that are produced by chemical or physical cross-linking of organic polymers in water by nanometer-scale objects, such as clays, silica nanoparticles, magnetic nanoparticles, or carbon nanotubes.[4,5] Owing to the reinforcement of the polymer matrix with nanoparticles, NC hydrogels show extraordinary mechanical strength and swelling/deswelling properties.[6] Additionally, current traditional tissue engineering scaffold approaches based on the control of cell behaviors and artificial tissue formation by suitable surface functionalization that closely mimics the natural extracellular matrix (ECM).[7] Therefore NC hydrogels are excellent candidates for 3D scaffolds for use in tissue engineering. Some research groups have reported the use of NC hydrogels in pharmaceutical and medical fields, such as wound dressing, cell cultivation, and bone remediation.[8] For example, recently Yang et al. described a new NC hydrogel from polyethylene glycol diacrylate and hydroxy mesoporous silica nanoparticles (MSNs-OH), which showed enhanced mechanical properties and promoted cellular affinity at the hydrogel surface.[8a] However, these studies are limited with respect to the inorganic material used in the NC hydrogel composition and the investigation of the obtained NC hydrogels for biochemical applications, because most of these studies represent the 2D cell growth on NC hydrogel surface[8a–c,f] and very few studies describe 3D cell encapsulation or cell growth in NC hydrogel scaffold.[8d,e]

Periodic mesoporous organosilicas (PMOs),[9,10] a class of functional organic–inorganic hybrid silica particles on the nanometer-scale, are a new alternative material as porous materials for new NC hydrogel formation owing to its unique properties, for example, high ordered mesopores, high specific surface area, narrow pore-size distributions, and easy surface functionalization.[9a,10c,11] In contrast to other hybrid inorganic–organic silica based materials, the organic units of the PMOs are implemented directly and homogeneously during the generation of the network of the PMO. Therefore, PMO can be functionalized efficiently and reproducibly during and after its preparation. Furthermore, its properties (magnetic, electronic, optical, and biological) can be controlled by the organic units, and the organic units as an intrinsic part of the pore wall network do not block the pores for further applications. Owing to these properties, PMOs should enhance the physical and biological properties of NC hydrogels. For example, homogeneously distributed organic functionalities at the surface of the PMO allow effective interactions with the polymeric network of the hydrogel to increase the mechanical properties of the respective NC material. At the same time, the modification of the PMOs surfaces with (bio)molecules may allocate an increasing density of contact points between, for example, cell and artificial surface. Therefore, the communication between the artificial material and the living systems is supported, resulting in a better and controlled adhesion of cells.[12] Moreover, the internal surface of PMOs can be functionalized or loaded specifically with guest molecules for imaging, drug release or mass transport. The tunable pore size of PMOs allows us to adapt the required space of the cavities to the sizes of the guest molecules. Although some advantages have been reported by us,[12a] and the groups of Lu, Yu, and Fröba[13] have described the use of functionalized PMOs for cell growth, drug release, and adsorption of bioactive molecules, the use of PMO in biotechnology is still very limited, and to the best of our knowledge PMOs have never been used for NC hydrogel formation as support for cell cultures.

In this respect, we present the preparation of new NC alginate hydrogels with multiple-functionalized PMOs (PMO-alginate) as nanometer-scale particles and nanocontainers, respectively, and the use of the respective NC hydrogels as models for 3D scaffolds by cell adhesion experiments. We demonstrate that PMO-alginate hydrogels show enhanced mechanical and biological properties compared to simple alginate hydrogel itself. Thus it was possible by using biomolecule functionalized PMO-alginate hydrogels

[*] Dr. N. S. Kehr, E. A. Prasetyanto, A. Galstyan
Physikalisches Institut and Center for Nanotechnology
Westfälische Wilhelms-Universität Münster
Heisenbergstrasse 11, 48149 Münster (Germany)
E-mail: seda@uni-muenster.de

K. Benson, Prof. H.-J. Galla
Institut für Biochemie, Westfälische Wilhelms-Universität Münster
Wilhelm-Klemm-Strasse 2, 48149 Münster (Germany)

B. Ergün
Department of Chemistry, Biochemistry Division
Hacettepe University, 06800 Ankara (Turkey)

[**] This work has been supported by DFG (SFB 858).

Supporting information for this article, including experimental and analytical details about the preparation and characterization of PMOs and gels, and details of the cell experiments, is available on the WWW under http://dx.doi.org/10.1002/anie.201206951.

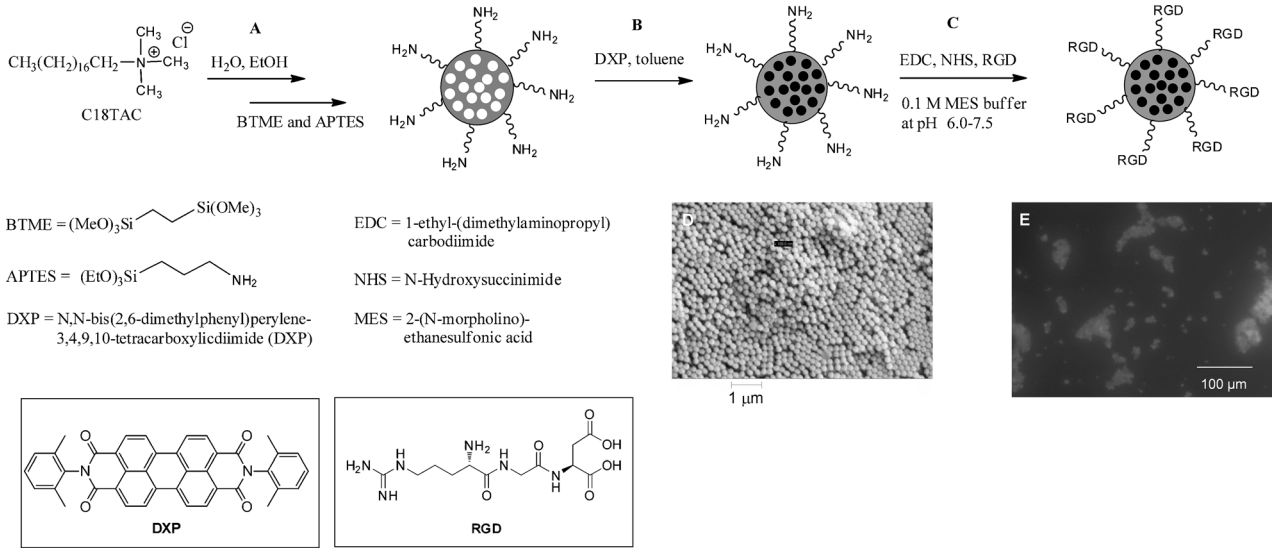

Figure 1. A) Synthesis of PMO-NH_2. B) DXP loading of PMO-NH_2 (^{DXP}PMO-NH_2). C) Functionalization of ^{DXP}PMO-NH_2 with RGD (^{DXP}PMO-RGD). D) SEM image of ^{DXP}PMO-RGD. E) Fluorescence microscopy image of ^{DXP}PMO-RGD (BP: 530–550 nm).

to increase the number of adhered alive cells in the NC hydrogel scaffold dramatically. Fluorescent dye molecules (DXP and Hoechst 33342) inserted inside the pores of the PMOs allows us on one hand to determine the position of the ^{DXP}PMO in the polymeric network with fluorescence microscopy, and on the other to demonstrate the use of PMO as nanocontainer to stain cells by release of Hoechst 33342.

Amino-functionalized spherical PMOs were synthesized according to a modified literature procedure.[14] Co-condensation of 3-aminopropyltriethoxysilane (APTES) and 1,2-bis(trimethoxysilyl)ethane (BTME) in the presence of cetyltrimethylammonium bromide (CTAB), a cationic surfactant, as mesoporous template resulted in amino-functionalized PMOs (PMO-NH_2; Figure 1 A). Then PMO-NH_2 were loaded with *N*,*N*′-bis(2,6-dimethylphenyl)perylene-3,4,9,10-tetracarboxylic diimide (DXP), a fluorescent dye molecule (Figure 1 B). Subsequently, DXP-loaded PMO-NH_2 (^{DXP}PMO-NH_2) was treated with the bioactive tripeptide Arg-Gly-Asp (RGD), one of the most effective peptide sequences for cell adhesion experiments,[15] in the presence of EDC (1-ethyl-3-(3-dimethylamino-propyl)carbodiimide) and NHS (N-hydroxysuccinimide) to finally obtain ^{DXP}PMO-RGD (Figure 1 C).

The obtained ^{DXP}PMO-RGD nanometer-scale particles were characterized by scanning electron microscopy (SEM; Figure 1 D), fluorescent microscopy (Figure 1 E), dynamic light scattering (DLS), small-angle X-ray scattering (SAXS), attenuated total reflection (ATR) IR spectroscopy, zeta-potential measurements, and thermogravimetric analyses (TGA) (for details, see the Supporting Information).

The ^{DXP}PMO-NH_2 and ^{DXP}PMO-RGD particles were then used to prepare the respective NC hydrogels with alginate (Supporting Information, Figure S6). A stock solution of alginate in water was cross-linked by adding a sonicated suspension of calcium D-gluconate monohydrate and the respective PMO particles. Further homogenization of the suspension led to a homogeneous calcium ion distribution and the crosslinking process (Figure 2 A; Supporting Information, Figure S6). The obtained NC hydrogel was frozen at −20 °C for 16 h and then lyophilized to get the respective PMO-alginate scaffolds for characterization (Figure 2 B).

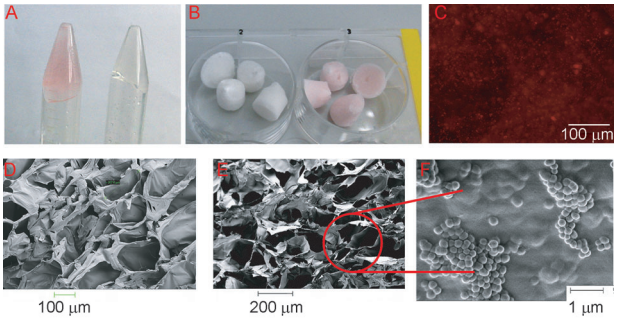

Figure 2. A) ^{DXP}PMO-RGD-alginate gel (left) and alginate gel (right). B) ^{DXP}PMO-RGD-alginate scaffold (left) and alginate scaffold (right) after freeze drying. C) Fluorescence microscopy images of ^{DXP}PMO-RGD-alginate scaffold (BP: 530–550 nm, red: DXP-loaded PMOs). D)–F) SEM images: D) alginate scaffold, E) ^{DXP}PMO-RGD-alginate scaffold, F) PMOs embedded in the polymer network.

The obtained ^{DXP}PMO-NH_2-alginate and ^{DXP}PMO-RGD-alginate scaffolds were characterized by SEM (Figure 2 D,E) and SAXS, rheological measurements, and fluorescence microscopy (for details, see the Supporting Information).

Cell adhesion experiments were first carried out by our new ^{DXP}PMO-RGD-alginate NC hydrogel (Figure 3 A). HeLa cells, an established cell line derived from cervical cancer, or primary porcine brain capillary endothelial cells (PBCEC), were seeded into the ^{DXP}PMO-RGD-alginate scaffold (Figure 3 A,C). As control experiments, the same cell line (HeLa) or primary cells (PBCEC) were seeded on ^{DXP}PMO-NH_2-alginate and alginate scaffolds, respectively (Figure B,D). After an incubation period (24 h at 37 °C), the obtained NC

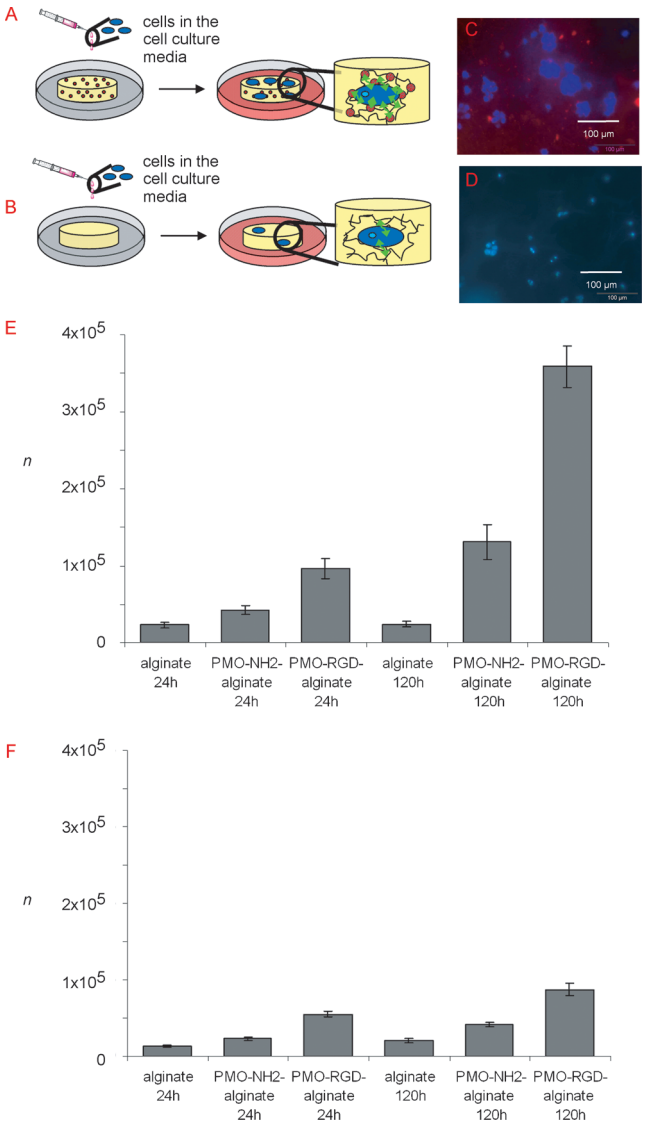

Figure 3. A) Cell adhesion in ^{DXP}PMO-RGD-alginate hydrogel. B) Cell adhesion in alginate hydrogel. C) Merge fluorescence microscopy image of HeLa cells adhered in ^{DXP}PMO-RGD-alginate gel (BP: 360–370 nm, BP: 530–550 nm, blue: DAPI-stained cells, red: DXP loaded PMO-RGD). D) Fluorescence microscopy image of HeLa cells adhered in alginate gel (BP: 360–370 nm, blue: DAPI-stained cells). E) The number *n* of live HeLa cells after 24 h/120 h incubation time (37 °C) in 1 mL of the respective gel scaffold (see Table 1). F) Number *n* of live endothelial cells after 24 h/120 h incubation time (37 °C) in 1 mL of the respective gel scaffold (see Table 1).

hydrogels were treated with trypsin and then dissolved in PBS with gentle mixing for a few seconds to extract alive cells, which were counted immediately with an automatic cell counter (Figure 3 E,F and Table 1). Our results showed that both HeLa and endothelial cells had higher affinity to our new ^{DXP}PMO-alginate NC hydrogels than to alginate hydrogel itself. We could extract about four times more live HeLa cells and endothelial cells from the ^{DXP}PMO-RGD-alginate NC hydrogel than from the alginate hydrogel. We also found close to twice as many live HeLa cells and live endothelial cells in the non-bioactive functionalized NC hydrogel

Table 1: Numbers ($\times 10^4$) of live HeLa/endothelial cells[a] at 37 °C in 1 mL gel composition.

	alginate	^{DXP}PMO-NH_2-alginate	^{DXP}PMO-RGD-alginate
HeLa cells [24 h]	2.30 ± 0.3 (14 %)	4.2 ± 0.6 (26 %)	9.6 ± 1.4 (44 %)
HeLa cells [120 h]	2.4 ± 0.4 (9 %)	13.1 ± 2.3 (19 %)	36.0 ± 2.7 (45 %)
Endothelial cells [24 h]	1.3 ± 0.2 (14 %)	2.3 ± 0.3 (16 %)	5.5 ± 0.4 (22 %)
Endothelial cells [120 h]	2.1 ± 0.2 (9 %)	4.1 ± 0.3 (20 %)	8.7 ± 0.8 (26 %)

[a] Incubation time is given in square barackets; cell viability is given in parentheses.

^{DXP}PMO-NH_2-alginate than in the simple alginate hydrogel. After an increase of the incubation time (120 h, 37 °C), the situation was more pronounced: while the amount of HeLa and endothelial cells in pure alginate gel were only marginally higher, we extracted about 3.5 times more live HeLa cells and about 1.6 times more endothelial cells from ^{DXP}PMO-NH_2-alginate and ^{DXP}PMO-RGD-alginate scaffolds, respectively, than after 24 h. Both cell types also showed higher affinity to ^{DXP}PMO-RGD-alginate (HeLa: 15 times more; endothelial cells: 4 times more) and ^{DXP}PMO-NH_2-alginate scaffolds (HeLa: 5 times more; endothelial cells: 2 times more) than to the simple alginate scaffold.

These results demonstrate that we can increase the number of alive cells and the cell viability in 3D alginate hydrogel networks by simple modification of the gel with functionalized nanometer-scale particles (for example, ^{DXP}PMO-RGD; see Table 1). Additionally, both the functionalization of the embedded PMO with bioactive groups (RGD) and the PMO particle itself promoted the cell affinity to the matrix of our PMO-alginate hydrogel. This may be caused by different macroscopic surface areas of the PMO-alginate NC hydrogel owing to the embedded PMO particles, in a similar fashion to the influence of 2D surface topography on cell behavior.[12,16] For example, Shiu et al. found that the number of cells attached to roughened biomaterials increased as the surface roughness increased[16a] and Park et al. showed that the adhesion, spreading, and differentiation of rat mesenchymal stem cells into the osteogenic lineage was highest on TiO_2 nanotubes than on plain TiO_2 surfaces.[16c] This may be attributed to the large surface area created by its roughness that allows a larger number of contact points between the cell and the material surface, resulting in a more efficient interaction, and therefore, for example in our case, to a better affinity of cells to the ^{DXP}PMO-alginate hydrogel (Figure 3 A,B).

The cell morpohology inside of the 3D ^{DXP}PMO-RGD-alginate scaffold was visualized by fluorescence microscopy. The cell membrane and cell nucleus of HeLa or endothelial cells were co-stained with Phalloidine Alexa Fluor 546 and 4′,6-diamidino-2-phenylindole-6-carboxamidine (DAPI), respectively. After 24 h incubation time, the cells inside the NC hydrogel were analyzed. The fluorescence microscopy images showed both cell types has spherical shape morphol-

ogy inside of the ^{DXP}PMO-RGD-alginate scaffold (Supporting Information, Figure S10).[17]

Finally, we carried out preliminary dye release experiments to prove the use of PMO particles as nanocontainers in 3D NC hydrogel scaffolds (Figure 4). Analogously as described above, we prepared Hoechst 33342 loaded PMO-RGD particles and the respective NC alginate hydrogel (^{Hoechst}PMO-RGD-alginate). Then we performed the respective cell experiments: HeLa cells were seeded into the ^{Hoechst}PMO-RGD-alginate scaffold. After an incubation period (24 h at 37 °C), the obtained NC hydrogels were washed twice with PBS^{++} (supplemented with 0.5 mM $MgCl_2$, 0.9 mM $CaCl_2$) and fixed with 4% paraformaldehyde (PFA) solution. The fluorescence microscopy image clearly showed blue stained Hela cell nuclei in the 3D NC hydrogel network caused by Hoechst 33342 dye, which was obviously released from the pores of the ^{Hoechst}PMO-RGD nanocontainers.

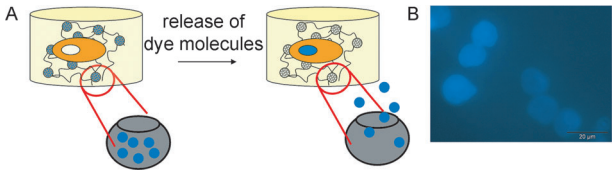

Figure 4. A) The release of dye molecules from pores of PMO. B) Fluorescence microscopy image of the nucleus of stained HeLa cells (BP:360–370 nm).

In conclusion, we have presented the preparation of new NC alginate hydrogels with bioactive molecule functionalized and fluorescence-dye-loaded PMOs. We demonstrated the beneficial effects of the embedded PMO particles of the respective NC hydrogel on its mechanical and biological properties. We also showed that the affinity of live cells, namely HeLa and endothelial cells, was up to four times higher using RGD functionalized PMO-alginate hydrogels than with simple alginate hydrogel, caused by both the nanometer-scale particle itself and its bioactive functionalization. Finally, as proof-of-principle, the use of the PMO in the NC hydrogel as nanocontainers was shown by the release of dye molecules from the pores of PMO to stain cell nuclei inside of the NC hydrogel. In the long term, applications of such NC hydrogels generated by the contribution of functionalized PMOs can be envisaged in many fields, for example tissue engineering, drug delivery, and catalysis.

Received: August 28, 2012
Revised: October 24, 2012
Published online: December 3, 2012

Keywords: cell adhesion · nanocomposite hydrogels · nanocontainers · mesoporous organosilica · three-dimensional scaffolds

[1] a) K. H. Liu, T. Y. Liu, S. Y. Chen, D. M. Liu, *Acta Biomater.* **2008**, *4*, 1038; b) K. Haraguchi, H. J. Li, *Angew. Chem.* **2005**, *117*, 6658; *Angew. Chem. Int. Ed.* **2005**, *44*, 6500; c) S. R. Sershen, G. A. Mensing, M. Ng, N. J. Halas, D. J. Beebe, J. L. West, *Adv. Mater.* **2005**, *17*, 1366; d) K. Haraguchi, K. Matsuda, *Chem. Mater.* **2005**, *17*, 931.

[2] a) S. M. Ong, C. Zhang, Y. C. Toh, S. H. Kim, H. L. Foo, *Biomaterials* **2008**, *29*, 3237; b) L. Yu, J. Ding, *Chem. Soc. Rev.* **2008**, *37*, 1473; c) J. D. Kretlow, L. Klouda, A. G. Mikos, *Adv. Drug Delivery Rev.* **2007**, *59*, 263; d) Y. Ding, Y. Hu, L. Zhang, Y. Chen, X. Jiang, *Biomacromolecules* **2006**, *7*, 1766; e) C. C. Lin, A. T. Metters, *Adv. Drug Delivery Rev.* **2006**, *58*, 1379; f) C. G. Williams, A. N. Malik, T. K. Kim, P. N. Manson, J. H. Elisseeff, *Biomaterials* **2005**, *26*, 1211.

[3] a) K. Haraguchi, R. Farnworth, A. Ohbayashi, T. Takehisa, *Macromolecules* **2003**, *36*, 5732; b) K. Haraguchi, T. Takehisa, S. Fan, *Macromolecules* **2002**, *35*, 10162.

[4] a) L. Petit, L. Bouteiller, A. Brulet, F. Lafuma, D. Hourdet, *Langmuir* **2007**, *23*, 147; b) D. Portehault, L. Petit, N. Pantoustier, F. Lafuma, D. Hourdet, *Colloids Surf. A* **2006**, *78*, 26.

[5] a) W. C. Lin, W. Fan, A. Marcellan, D. Hourdet, C. Creton, *Macromolecules* **2010**, *43*, 2554; b) M. A. Cohen Stuart, *Colloid Polym. Sci.* **2008**, *286*, 855; c) S. H. Nair, K. C. Pawar, J. P. Jog, M. V. Badiger, *J. Appl. Polym. Sci.* **2007**, *103*, 2896; d) Y. Kaneko, S. Sato, J. Kadokawa, N. Iyi, *J. Mater. Chem.* **2006**, *16*, 1746; e) Y. Xiang, Z. Peng, D. Chen, *Eur. Polym. J.* **2006**, *42*, 2125; f) X. Zhao, X. Ding, Z. Deng, Z. Zheng, Y. Peng, X. Long, *Macromol. Rapid Commun.* **2005**, *26*, 1784; g) K. V. Durmea, B. V. Melea, W. Loosb, F. E. D. Prez, *Polymer* **2005**, *46*, 9851; h) K. Haraguchi, H. J. Li, *J. Network Polym. Jpn.* **2004**, *25*, 81; i) K. M. Kim, Y. Chujo, *J. Mater. Chem.* **2003**, *13*, 1384.

[6] a) Q. Wang, J. L. Mynar, M. Yoshida, E. Lee, M. Lee, K. Okuro, K. Kinbara, T. Aida, *Nature* **2010**, *463*, 339; b) C. M. Paranhos, B. G. Soares, R. N. Oliveira, L. A. Pessan, *Macromol. Mater. Eng.* **2007**, *292*, 620; c) K. Haraguchi, T. Takehisa, *Adv. Mater.* **2002**, *14*, 1120.

[7] a) A. Khademhosseini, J. P. Vacanti, R. Langer, *Sci. Am.* **2009**, *300*, 64; b) R. Langer, J. P. Vacanti, *Science* **1993**, *260*, 920.

[8] a) S. Yang, J. Wang, H. Tan, F. Zeng, C. Liu, *Soft Matter* **2012**, *8*, 8981; b) A. K. Gaharwar, S. A. Dammu, J. M. Canter, C. J. Wu, G. Schmidt, *Biomacromolecules* **2011**, *12*, 1641; c) A. K. Gaharwar, P. Schexnailder, V. Kaul, O. Akkus, D. Zakharov, S. Seifert, G. Schmidt, *Adv. Funct. Mater.* **2010**, *20*, 429; d) C.-W. Chang, A. van Spreeuwel, C. Zhang, S. Varghese, *Soft Matter* **2010**, *6*, 5157; e) Y. S. Pek, A. C. A. Wan, A. Shekaran, L. Zhuo, J. Y. Ying, *Nat. Nanotechnol.* **2008**, *3*, 671; f) Y. Hou, A. R. Matthews, A. M. Smitherman, A. S. Bulick, M. S. Hahn, H. Hou, A. Han, M. A. Grunlan, *Biomaterials* **2008**, *29*, 3175.

[9] a) S. Inagaki, S. Guan, Y. Fukushima, T. Ohsuna, O. Terasaki, *J. Am. Chem. Soc.* **1999**, *121*, 9611; b) T. Asefa, M. J. MacLachlan, N. Coombs, G. A. Ozin, *Nature* **1999**, *402*, 867; c) B. J. Melde, B. T. Holland, C. F. Blanford, A. Stein, *Chem. Mater.* **1999**, *11*, 3302.

[10] a) F. Hoffmann, M. Cornelius, J. Morell, M. Fröba, *Angew. Chem.* **2006**, *118*, 3290; *Angew. Chem. Int. Ed.* **2006**, *45*, 3216; b) B. Hatton, K. Landskron, W. Whitnall, D. Perovic, G. A. Ozin, *Acc. Chem. Res.* **2005**, *38*, 305; c) W. J. Hunks, G. A. Ozin, *J. Mater. Chem.* **2005**, *15*, 3716.

[11] W. Guo, X. S. Zhao, *Microporous Mesoporous Mater.* **2005**, *85*, 32.

[12] a) K. Benson, Y. E. A. Prasetyanto, H.-J. Galla, N. S. Kehr, *Soft Matter* **2012**, *8*, 10845; b) J. El-Gindi, K. Benson, L. De Cola, H.-J. Galla, N. S. Kehr, *Angew. Chem.* **2012**, *124*, 3776; *Angew. Chem. Int. Ed.* **2012**, *51*, 3716; c) N. S. Kehr, J. El-Gindi, H. J. Galla, L. De Cola, *Microporous Mesoporous Mater.* **2011**, *144*, 9; d) N. S. Kehr, K. Riehemann, J. El-Gindi, A. Schäfer, H. Fuchs, H. J. Galla, L. De Cola, *Adv. Funct. Mater.* **2010**, *20*, 2248.

[13] a) M. Beretta, J. Morell, P. Sozzoni, M. Fröba, *Chem. Commun.* **2010**, *46*, 2495; b) J. Wan, K. Qian, J. Zhang, F. Liu, Y. Wang, P. Yang, B. Liu, C. Yu, *Langmuir* **2010**, *26*, 7444; c) C. X. Lin, S. Z. Qiao, C. Z. Yu, S. Ismadji, G. Q. Lu, *Microporous Mesoporous*

Mater. **2009**, *117*, 213; d) W. Cai, I. R. Gentle, G. Q. Lu, J. J. Zhu, A. Yu, *Anal. Chem.* **2008**, *80*, 5401; e) S. Z. Qiao, H. Djojoputro, Q. H. Hu, G. Q. Lu, *Prog. Solid State Chem.* **2006**, *34*, 249; f) S. Z. Qiao, C. Z. Yu, W. Xing, Q. H. Hu, H. Djojoputro, G. Q. Lu, *Chem. Mater.* **2005**, *17*, 6172.

[14] W. Guo, J. Wang, S. J. Lee, F. Dong, S. S. Park, C. S. Ha, *Chem. Eur. J.* **2010**, *16*, 8641.

[15] M. D. Pierschbacher, E. Ruoslahti, *Nature* **1984**, *309*, 30.

[16] a) J. Y. Shiu, C. W. Kuo, W. T. Whang, P. Chen, *Lab Chip* **2010**, *10*, 556; b) L. Ferreira, J. M. Karp, L. Nobre, R. Langer, *Cell Stem Cell Rev.* **2008**, *3*, 136; c) J. Park, S. Bauer, K. von der Mark, P. Schmuki, *Nano Lett.* **2007**, *7*, 1686; d) T. Sun, H. Tan, D. Han, Q. Fu, L. Jiang, *Small* **2005**, *1*, 959.

[17] a) M. Leung, F. M. Kievit, S. J. Florczyk, O. Veiseh, J. Wu, J. O. Park, M. Zhang, *Pharm. Res.* **2010**, *27*, 1939; b) X. Zhou, R. G. Rowe, N. Hiraoka, *Genes Dev.* **2008**, *22*, 1231.

